R.M. BALABAI

Kryvyi-Rih Pedagogical Institute, Kryvyi-Rih National University, Department of Physics
(54, Gagarin Ave., Kryvyi Rih 50086, Ukraine; e-mail: oks_pol@cabletv.dp.ua)

PACS 73

ELECTRONIC PROPERTIES OF FUNCTIONALIZED GRAPHENE NANORIBBONS

Distributions of valence electron density in and the electron energy spectrum of graphene nanoribbons covered with hydrogen, fluorine, or oxygen atoms have been calculated ab initio in the framework of the density functional and pseudopotential theories. The emergence of a forbidden gap for graphene nanoribbons with zigzag edges and 9.23 Å in width and its absence in an unconfined graphene plane are shown. The forbidden gap is demonstrated to decrease, as the graphene nanoribbon width increases. For graphene nanoribbons with hydrogen-decorated edges, the energy gap disappears. The interaction between a hydrogen atom and carbon atoms in the graphene nanoribbon plane that are coordinated in accordance with the sp^2-hybridization is shown to induce local changes of the hybridization to the sp^3 type.

K e y w o r d s: graphene nanoribbons, electron density functional method, pseudopotential method.

1. Introduction

The influence of edges in graphene nanoribbons (GNRs) on their electron structure is rather strong, so that the chemistry of GNRs considerably differs from that of massive graphene. This problem has attracted a close attention since the first works by Louie *et al.* [1] had been published, in which a semimetallic ferromagnetic state of zigzag graphene edges was predicted on the basis of the results of calculations in the framework of the electron density functional method. The majority of works on this topic are calculation ones – see, e.g., works [2–6] – and are aimed at the determination of factors that govern the electron structure of GNRs and change their conducting, magnetic, heat-conducting, and transport properties.

Graphene nanoribbons are prolonged strips of graphene with a finite width. They can be produced by cutting the graphene plane along certain directions or using the lithographic methods [7–9]. Owing to a lattice structure of graphenes, two prototypes of their edges are possible. These are the armchair (Fig. 1, *b*) and zigzag (Fig. 1, *c*) ones with a difference of 30° between the directions of their orientations. Besides two indicated "perfect" edge shapes, more complicated GNR edge geometries combined of armchair and zigzag fragments can also be realized.

The atomic structures of GNRs with armchair and zigzag edges and the corresponding unit cells are sketched in Fig. 2. According to conventional rules [10], GNRs with both armchair and zigzag edges are classed by the number N of dimer or zigzag lines, respectively, across the strip width, as is shown in Fig. 2.

In 2010, Cai *et al.* [11] succeeded in synthesizing an armchair GNR with defect-free edges and a definite width of 7 lines. It became a seminal event in the domain of activities aimed at the creation of substances with predicted properties. At the same time, a similar synthesis for other GNRs turned out not so successful. A typical lithographic manufacture of GNRs includes their treatment with oxygen plasma, which makes the passivation of GNR edges not only by hydrogen very probable. In this case, it is very important to know how the edge and surface functionalizations affect the physical properties of GNRs. On the other hand, the functionalization can be carried out purposely in order to change GNR properties for possible practical applications.

In general, the influence of the real edges of GNRs, their width, and the state of their surface on the electronic GNR properties is not clear enough, so that those very important problems need to be researched further.

2. Objects and Methods of Research

In this work, the electronic properties of functionalized GNRs are studied by carrying out *ab initio* calculations with the use of electron density functional
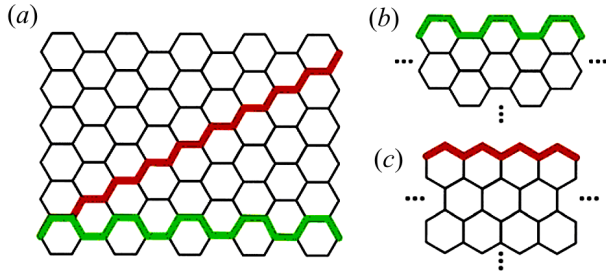
Fig. 1. Lattice structure of graphene (*a*) with distinguished armchair and zigzag directions. Graphene nanoribbons (GNRs) are cut out from an ideal graphene plane along two highly symmetric directions, being called armchair (aGNRs) (*b*) and zigzag (zGNRs) graphene nanoribbons (*c*)
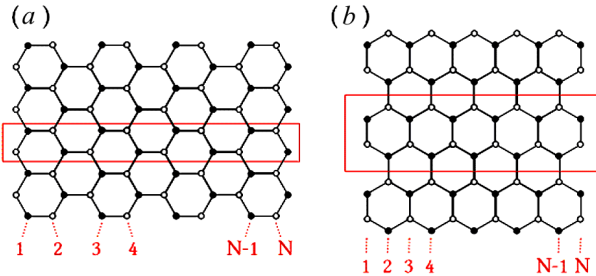
Fig. 2. Carbon *N*-aGNRs (*a*) and *N*-zGNRs (*b*) composed of *N* armchair or zigzag lines, respectively. White and black circles identify carbon atoms related to two different sublattices, A and B. Rectangles confine unit cells in corresponding GNRs. The enumerated atoms correspond to the number of zigzag chains or dimer lines across the nanoribbon width

and pseudopotential methods. The results were obtained with the help of author's program code [12, 13]. The latter realizes either the algorithm of quantummechanical dynamics if the variables describing the electron and nuclear subsystems of a multiatomic structure are optimized simultaneously, or the algorithm of self-consistent solution of Kohn–Sham equations if only the electron variables are determined for fixed atomic cores.

The ground states of electron-nuclear systems were determined by solving self-consistently the Kohn–Sham equations, i.e., only the electron variables were determined, by assuming the atomic core to be fixed. Following the Kohn–Sham approach, the electron density is written down in terms of occupied orthonormalized one-particle wave functions,

$$n(\mathbf{r}) = \sum_i |\psi_i(\mathbf{r})|^2. \tag{1}$$

The point on the potential energy surface in the Born–Oppenheimer approximation was determined as a minimum of the energy functional with respect to the wave functions,

$$E\left[\{\psi_i\}, \{\mathbf{R}_j\}, \{\alpha_\nu\}\right] = \sum_i \int_\Omega d^3r \psi_i^*(\mathbf{r}) \times$$

$$\times \left[-\frac{\hbar^2}{2m}\nabla^2\right] \psi_i(\mathbf{r}) + U\left[\{n(\mathbf{r})\}, \{\mathbf{R}_j\}, \{\alpha_\nu\}\right], \tag{2}$$

where the notation $\{\mathbf{R}_j\}$ means the coordinates of core atoms, and $\{\alpha_\nu\}$ includes all possible external influences on the system.

In the standard formulation, the minimization of the energy functional (2) with respect to one-particle orbitals that obey additional orthonormalization conditions brings about one-particle Kohn–Sham equations,

$$\left\{-\frac{\hbar^2}{2m}\nabla^2 + \frac{\partial U}{\partial n(\mathbf{r})}\right\} \psi_i(\mathbf{r}) = \varepsilon_i \psi_i(\mathbf{r}). \tag{3}$$

The distribution of electrons over the energy bands in the Γ-state of structures concerned was obtained numerically by calculating the derivative $\lim_{\Delta E \to 0}(\Delta N/\Delta E)$, where ΔN is the number of allowed states in the energy interval ΔE. The required quantities were calculated in the course of diagonalization of the Kohn–Sham matrix for the one-particle energy spectrum, in which the number of values was controlled by the size of the wave function expansion. According to the ideology of the electron density functional theory, the states occupied at $T = 0$ K (the states in the valence bands and the state in the energy gap associated with defects) were found. This allows us to determine the position of the Fermi level as that of the last occupied state. The number of occupied states was put equal to half a number of electrons, because the electron spin was neglected.

The algorithm of calculations supposed the presence of the translational symmetry for the atomic system under study. Therefore, an artificial supercell of tetragonal type was created first. (Its parameters and atomic basis were regarded as the research objects.) In such a way, the translational periodicity in three directions was introduced into the atomic system. In other words, an artificial three-dimensional periodic system was created. It consisted of either graphene ribbons repeated in three directions and of graphene
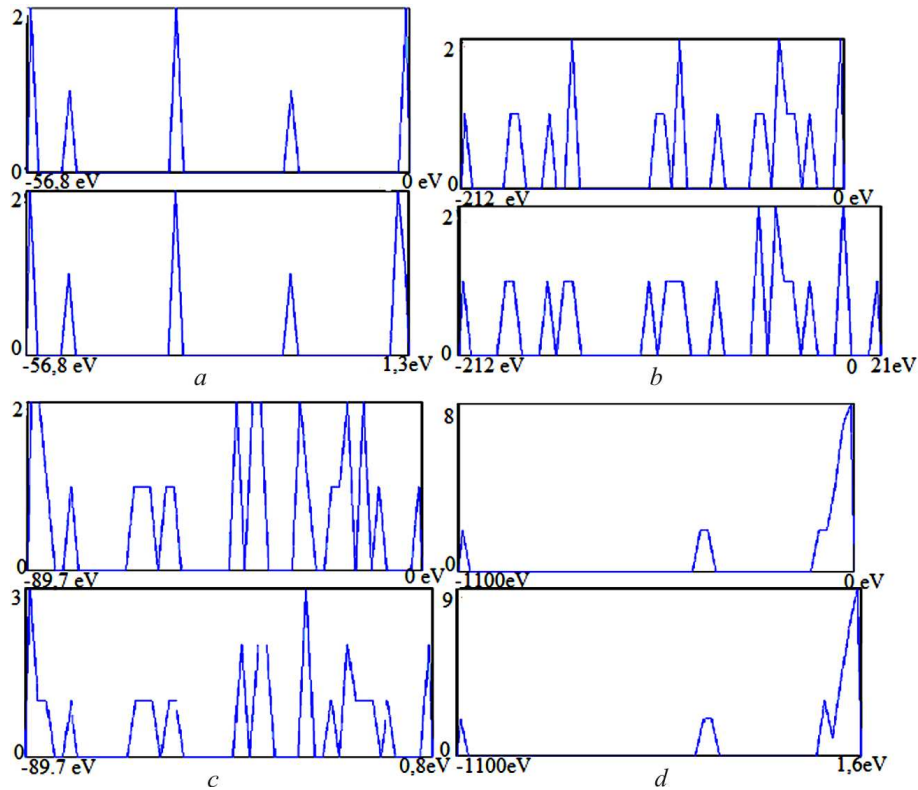
Fig. 3. Distributions of states at the Γ-point of the Brillouin zone in a superlattice that simulates the graphene plane (a), the 5-zGNR (b), the 7-zGNR (c), and the 7-zGNR with hydrogen-decorated edges (d). The upper distribution in the group corresponds to the valence band states and the lower one to the valence band states and the next allowed state. The energy in electron volts is reckoned along the abscissa axis, and the number of states is shown on the ordinate axis

planes repeated in two ones. But the cell parameters and the atomic coordinates in the basis were so selected that there was no interaction between spatially repeated ribbons (planes), which allowed a single infinite graphene ribbon (a plane) to be analyzed.

3. Results of Calculations and Their Discussion

In order to study the evolution of the electronic properties of graphene-like structures when H, F, and O atoms join them, the atomic bases of a primitive cell in an artificial superlattice were created to simulate a nanoribbon that is infinite in one direction. The cell parameters were so selected to simulate the ribbon with infinite length in the X-direction, the confinement of the ribbon by so-called edges in the Y-direction, and free surfaces in the Z-direction. The confinement of a graphene plane in one direction,

the nanoribbon edges terminated by hydrogen atoms, and the adsorption of hydrogen, fluorine, or oxygen atoms on the surface change the electron structure of the material.

While carrying out researches, five or seven zigzag chains of carbon atoms were taken, which determined the zGNR width (N-zGNR, $N = 5$ or 7, see Fig. 2). For the sake of comparison, the calculations were carried out for an infinite graphene plane as well, using the superlattice technique. In so doing, the parameters of the primitive cell were so selected to simulate an infinite plane in the X- and Y-directions, and free surfaces in the Z-direction. The atomic bases created for all calculation objects had a symmetry that contained only two operations in its point group: the identical and inverse transformations. Using author's software, the electron spectrum for the Γ-point of the Brillouin zone in the three-dimensional superlattice, the spatial distributions of valence electron density,
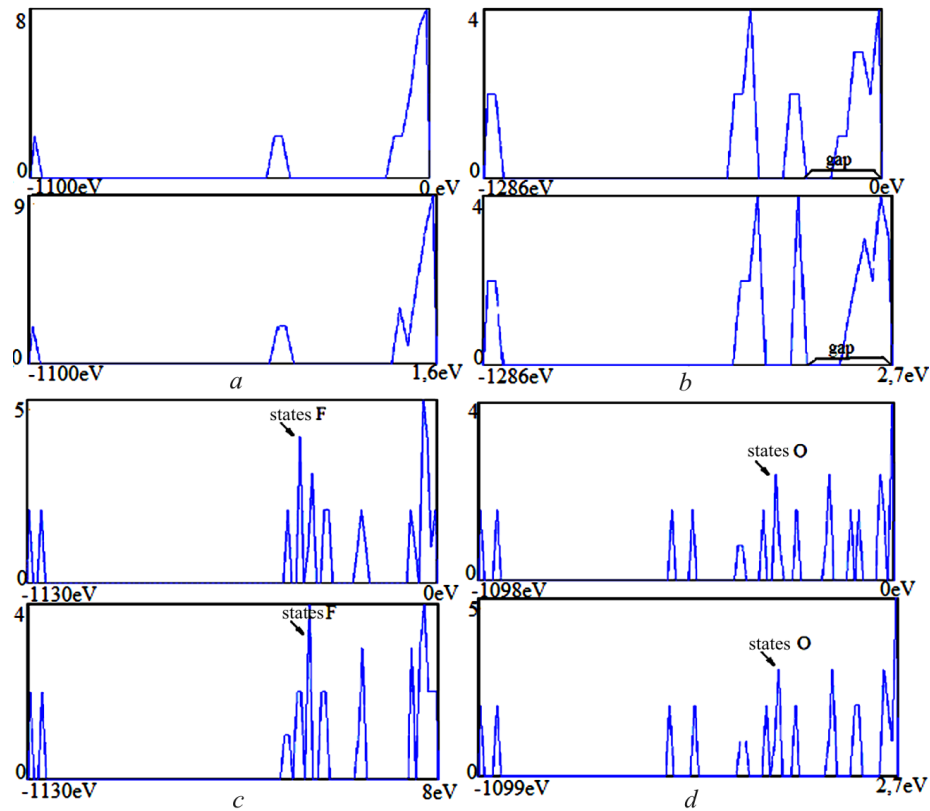
Fig. 4. Distributions of states at the Γ-point for the 7-zGNR with H-decorated edges (*a*); the same GNR as in panel (*a*), but with two additional H atoms located above the neighbor C atoms on the different sides from the GNR plane (*b*); for the same GNR as in panel (*b*), but with two additional F atoms located over C atoms on the different sides from the GNR plane at positions that are the nearest to H atoms (*c*); for the same GNR as in panel (*c*), but with two additional O atoms instead of F ones (*d*). In each group of distributions, the upper distribution corresponds to valence band states, and the lower one to valence band states and the next allowed state. The energy in electron volts is reckoned along the abscissa axis, and the number of states is shown on the ordinate axis

and their cross-sections were calculated. Attention should be paid to the fact that the Γ-point for superlattice calculations has the sense of the Baldereschi mean-value point [13], which represents all vectors in the Brillouin zone.

In Fig. 3, the distributions of valence electron states calculated for various graphene-like structures are shown. In order to determine whether the energy gap exists, two distributions are depicted for each of the studied structures. One of them describes only states occupied at $T = 0$ K (the right energy limit of the distribution defines the Fermi level and is designated as 0 eV), the other also includes the next free state allowed at $T = 0$ K. This state in the conduction band is either unseparated from the previous occupied state within the plot resolution or separated by

an appreciable forbidden energy gap. One can observe the emergence of the energy gap in the 5-zGNR 9.23 Å in width (Fig. 3, *b*) and its absence in the case of unconfined graphene plane (Fig. 3, *a*). For the 7-zGNR 13.42 Å in width (Fig. 3, *c*), additional states associated with dangling bonds of C atoms at the ribbon edges are located very close to the conduction band in this GNR (in Fig. 3, *c*, the last occupied state and the first free one merged together for the given plot resolution), i.e. the forbidden gap diminishes, as the zGNR width increases. For GNRs with hydrogen-decorated edges (Fig. 3, *d*), the forbidden gap disappears.

In Fig. 4, the distributions of valence electron states at the Γ-point of the Brillouin zone in the superlattice for the 7-zGNR with hydrogen-decorated edges
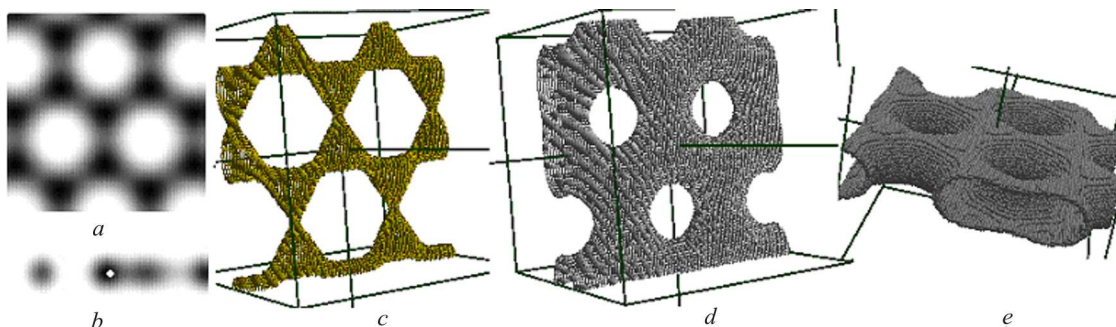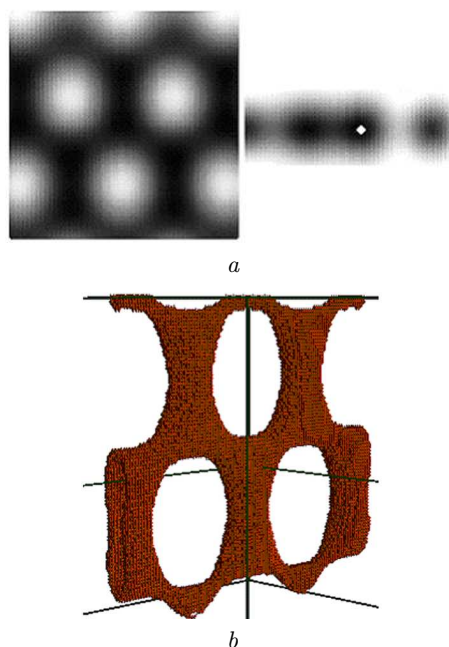
Fig. 5. Longitudinal (*a*) and transverse (*b*) cross-sections of the spatial distribution of valence electron density over an unconfined graphene plane drawn through the centers of atoms, spatial distribution of valence electron density within the interval of 0.6–0.7 of the maximum value (*c*); the same as in panel (*c*), but for the interval of 0.1–0.2 of the maximum value exposed in different perspectives (*d*) and (*e*)

are exhibited for the following conditions of atomic adsorption on the GNR surface.

(i) There are two hydrogen atoms per unit cell. They are adsorbed at a distance of 1.07 Å from the graphene plane and located above the neighbor carbon atoms on the different sides from the plane. For the selected size of the unit cell, such a number of H atoms in the atomic basis corresponds to a concentration of adsorbed hydrogen atoms of 14.3%.

(ii) There are four atoms per unit cell. Two of them are hydrogens, which are located as was described above. The two others are fluorine or oxygen atoms with a concentration of 14.3%, which are distanced from the GNR plane by 1.41 or 1.43 Å, respectively, being located at the positions that are the nearest to H's on the different sides from the plane. The total concentration of atoms adsorbed on the GNR surface equaled 28.6% in this case.

For the sake of comparison, Fig. 4, *a* exhibits the calculated distribution for the 7-zGNR with hydrogen-decorated edges but clean surfaces. In Figs. 4, *c* and *d*, the arrows point to the states of *p*-electrons in O and F atoms. The analysis of the presented distributions brings us to a conclusion that the adsorption of hydrogen to a concentration of 14.3% onto the 7-zGNR devastates additional electron states in the graphene ribbon, which are densely grouped into a band near the conduction band bottom (see the group of states on the right-hand side in Fig. 4, *b*). The additional adsorption of F and O atoms to a concentration of 14.3% on the 7-zGNR surfaces previously hydrogenated to a concentration of 14.3% leads to a separation of additional states in the upper section of the forbidden gap.
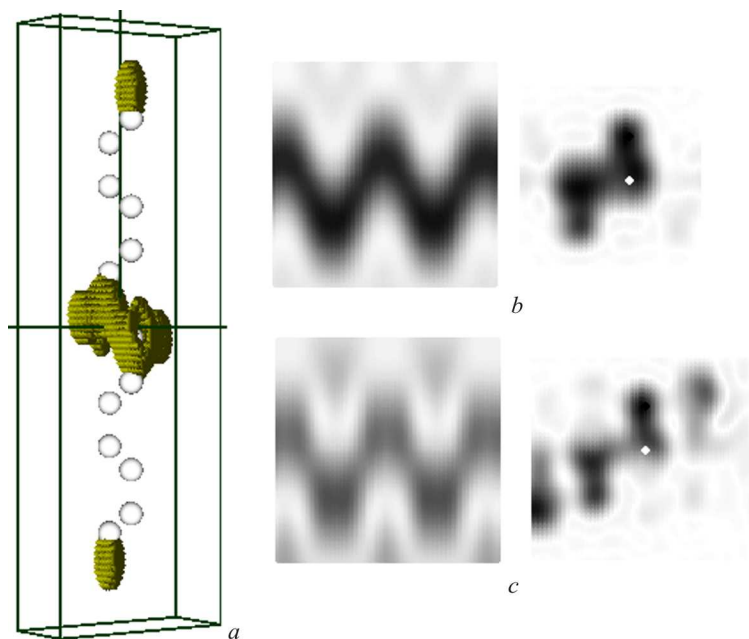

Fig. 6. Distributions of valence electron density for the 5-zGNR: longitudinal cross-section through the centers of atoms (left panel) and transverse cross-section in a vicinity of the C atom the most distant from the edges (right panel) (*a*); spatial distribution of valence electron density within the interval of 0.8–0.9 of the maximum value for the C atom the most distant from the edges (*b*)

In order to study how the concentration of hydrogen atoms adsorbed on the surface of 7-zGNR with hydrogen-decorated edges affects the electronic properties of GNR, a unit cell with a larger number of atoms has been created. In particular, it included 42 carbon atoms against 14 ones used earlier, which
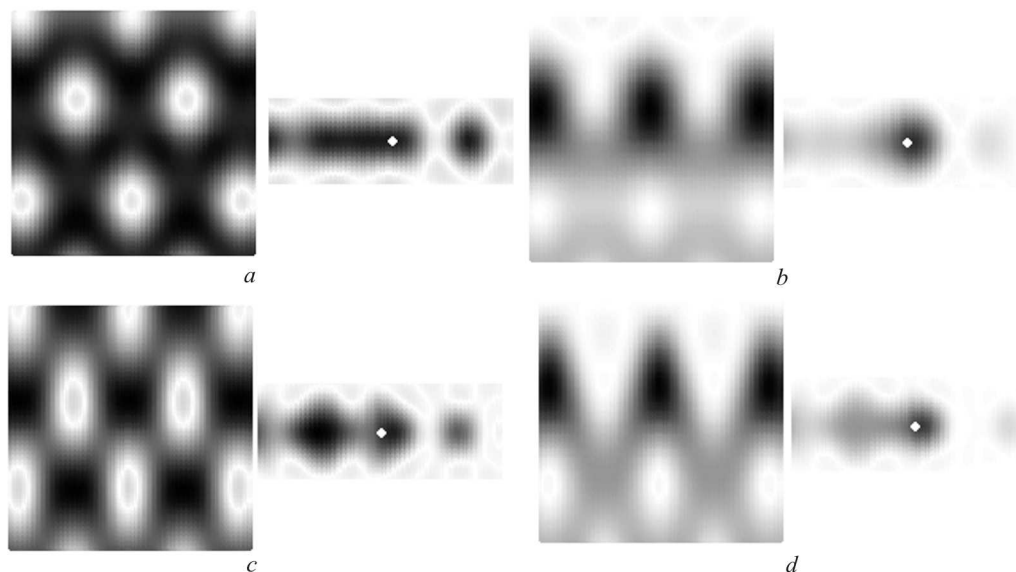
Fig. 7. Longitudinal and transverse cross-sections of the spatial distributions of valence electron density for the 5-zGNR with hydrogen-decorated edges (*a*) in a vicinity of the C atoms the most distant from the edges and (*b*) in a vicinity of the C atoms that confine the ribbon and interact with hydrogen atoms. Panels (*c*) and (*d*) illustrate the same distributions for the same positions of atoms described above, but for the 7-zGNR

Fig. 8. Distribution of valence electron density within the interval of 0.5–0.6 of the maximum value in a unit cell of the 7-zGNR with H-decorated edges and adsorbed H atoms (to a concentration of 14.3%) at positions located on the different sides from the graphene plane over the neighbor C atoms that are the most distant from the edges (*a*). Longitudinal and transverse cross-sections of the spatial distribution in a vicinity of the C atom with a hydrogen atom being adsorbed above (*b*) and in a vicinity of the same C atom, but in the GNR with an additionally adsorbed O atom at the position that is nearest to this C atom (above the neighbor carbon atom) (*c*)

394
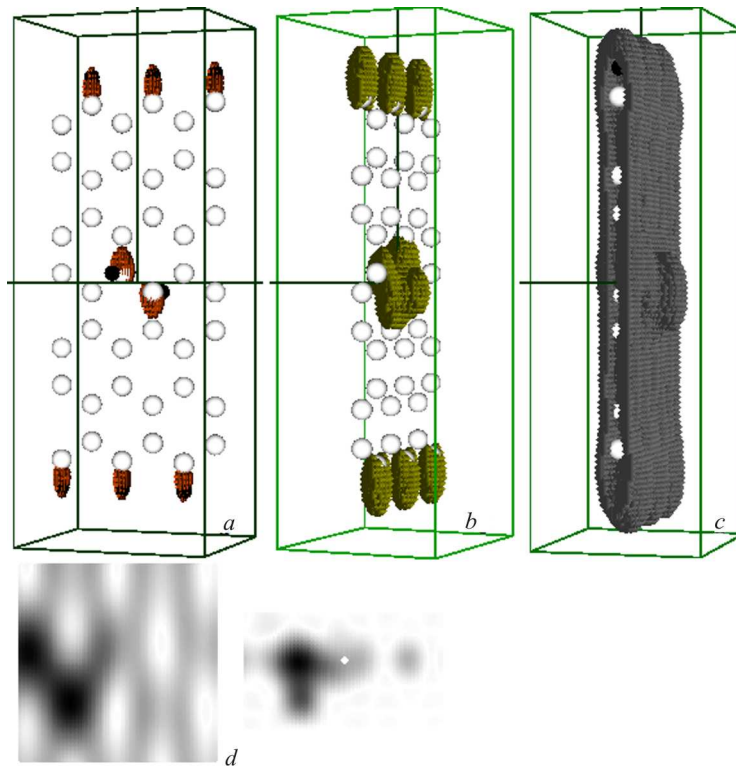
Fig. 9. Distribution of valence electron density within the interval of 0.8–0.9 of the maximum value in a unit cell of the 7-zGNR with H-decorated edges and adsorbed H atoms (to a concentration of 4.8%) at positions located on the different sides from the graphene plane over the neighbor C atoms that are the most distant from the edges(*a*). The same as in panel *a*, but for the concentration intervals of 0.5–0.6 and 0.1–0.2, respectively, of the maximum value (*b*) and (*c*). Longitudinal and transverse cross-sections of the spatial distribution in a vicinity of the C atom with a hydrogen atom being adsorbed above (*d*)

allowed the calculated concentration of adsorbed hydrogens to be reduced to 4.8%. Comparing the magnitudes of energy ranges for states occupied by valence electrons at $T = 0$ K in the 7-zGNRs with hydrogen-decorated edges but free of adsorbed hydrogen atoms, and with hydrogen coatings to concentrations of 4.8, 14.3, and 100%, a conclusion can be drawn – on the basis of broadening of those ranges in GNRs hydrogenated to concentrations of 4.8 and 14.3% with respect to the 0%-concentration values – that the states leave the valence band and penetrate into the energy gap, which is more significant for GNRs with a higher hydrogen concentration. A complete coating of 7-zGNR surfaces with hydrogens strongly narrows the interval of allowed states, which reduces the total energy of the system and increases its inertness.

The spatial distributions of valence electron density and their cross-sections at various points of the studied graphene structures are depicted in Figs. 5 to 9. The distribution in an unconfined graphene plane is uniform over the plane (Fig. 5), in contrast to the distributions in GNRs. The following characteristic features can be indicated for the latter. For non-decorated GNRs, which are confined in one direction, the non-uniformity of the distributions is determined in two mutually perpendicular directions, along the infinite ribbon and along the direction of its confinement (cf. Figs. 5 and 6). For GNRs with hydrogen-decorated edges, this non-uniformity becomes even more pronounced (Fig. 7).

Adsorption of hydrogen atoms by carbon ones, which belong to the graphene plane and are completely coordinated in correspondence with the sp^2-hybridization, gives rise to the change from this hybridization to the sp^3-one. This can be seen from a distribution typical of diamond-like structures, which was formed in the GNR plane un-

der hydrogen atoms (Figs. 8, *a* and *b*). The electron density redistribution of such a type consisting in the appearance of a cord with a higher concentration was observed for the 7-zGNRs, which adsorbed so many hydrogen atoms that the regions in which the electron density in graphene changed under hydrogens became overlapped (a hydrogen concentration of 14.3%). If hydrogen atoms were adsorbed to lower concentrations – e.g., 4.8% – and the regions of electron density in graphene under hydrogens were not overlapped, no change of the hybridization type was observed (Fig. 8).

Additional adsorption of atoms of a different kind, e.g., fluorines or oxygens, on the preliminary hydrogenated GNR surface into positions that are the nearest to hydrogen atoms (according to the authors of work [14], such adsorption is the most beneficial, because this GNR site is the most perturbed one) restores the hybridization type of carbon electrons back to sp^2 (see Fig. 9, *c*).

The authors of works [15, 16] predicted the appearance of effective partial bonds of the sp^3 type in ribbon graphene structures with damaged chemical sp^2 groups. The cited authors assert that the presence of such point defects can be used as a useful engineering approach to the creation of a new class of carbon semiconductors, which can be used in nano-electronics, in particular, for the creation of field-effect transistors. A similar transformation of the triangular coordination of carbon atoms into that close to the tetrahedral one, which takes place in fluorinated nanotubes, was also observed in single-wall clean nanotubes [17]. The latter transformation is possible only if the sp^2-hybridization of valence states of carbon atoms in initial tubes is replaced by the sp^3-one in nanotubes with fluorine atoms attached normally to the surface. Such an arrangement of fluorine atoms on the nanotube wall after the fluorination process was observed experimentally [18]. Having analyzed the structure of x-ray absorption spectra obtained for the fluorine–carbon phase, the cited authors drew conclusion that, at the fluorination of a carbon nanotube, the fluorine atom does not substitute the carbon one, but becomes bound to it normally to the wall by forming a $C2p_z$ state and, hence, forming a spatial rather than plane configuration for the carbon atom.

4. Conclusions

The methods of electron density functional and pseudo-potential theories were used to calculate, *ab initio*, the distributions of valence electron densitys and the energy spectra of electrons for graphene nanoribbons decorated with hydrogen, fluorine, or oxygen atoms.

The emergence of the energy gap in the 5-zGNR (23 Å in width) and its absence in the unconfined graphene plane were demonstrated. The forbidden gap width decreases with the growth of the GNR width to that of 7 atomic chains (13.42 Å). For GNRs with hydrogen-decorated edges, the energy gap disappears.

Adsorption of hydrogen atoms to a concentration of 14.3% by the surface of 7-zGNR devastates additional electron states, which are densely grouped into a band near the conduction band bottom. If the 7-zGNR surface is preliminarily hydrogenated to a concentration of 14.3%, it additionally adsorbs F or O atoms to a concentration of 14.3%, the additional states in the upper section of the energy gap become separated.

The conclusion was drawn concerning the separation of states from the valence band and their removal into the energy gap in GNRs hydrogenated to H concentrations of 4.8 and 14.3% in contrast to non-hydrogenated ones, with the effect being more pronounced for GNRs with a higher hydrogen concentration. At the same time, the full coating of 7-zGNR surfaces with hydrogen strongly narrows the interval of allowed states, which reduces the total energy of the system and increases its inertness.

The distribution of valence electron density was demonstrated to be uniform over the unconfined graphene plane. On the contrary, the following characteristic features can be distinguished for those distributions in GNRs. For non-decorated GNRs confined in one direction, the non-uniform distributions are observed in two mutually perpendicular directions, namely, along the infinite ribbon and along the direction of its confinement. For hydrogen-decorated GNRs, this non-uniformity becomes even more pronounced.

Interaction between hydrogen atoms and carbon atoms coordinated in the GNR plane according to the sp^2-hybridization was shown to result in local changes of the hybridization to the sp^3 type.

A transformation of the electron density into a continuous "cord" with a higher concentration value was observed for 7-zGNRs, on which so many hydrogens were adsorbed that the regions of electron density transformation in graphene under hydrogen atoms became overlapped (a hydrogen concentration of 14.3%). If hydrogen atoms were adsorbed to a lower concentration (4.8%) and the regions of electron density transformation in graphene under hydrogens did not overlapped, no change in the hybridization type was observed.

Additional adsorption of different atoms – e.g., fluorines or oxygens – on already hydrogenated GNRs into positions that are the closest to hydrogen atoms was shown to restore the type of hybridization for carbon electrons back to the sp^2 one.

1. Y.-W. Son, M.L. Cohen, and S.G. Louie, Nature **444**, 347 (2006).
2. H. Raza, J. Phys. Condens. Matter **23**, 382203 (2011).
3. A. Dasgupta, S. Bera, F. Evers, and M.J. van Setten, Phys. Rev. B **85**, 125433 (2012).
4. H. Karamitaheri, N. Neophytou, M. Pourfath, R. Faez, and H. Kosina, J. Appl. Phys. **111**, 054501 (2012).
5. P. Wagner, C.P. Ewels, V.V. Ivanovskaya, P.R. Briddon, A. Pateau, and B. Humbert, Phys. Rev. B **84**, 134110 (2011).
6. L.T. Nguyen *et al.*, J. Phys. Condens. Matter **23**, 295503 (2011).
7. A. Javey, *Carbon Nanotube Electronics* (Springer, New York, 2009).
8. M.Y. Han, B. Ozylmaz, Y. Zhang, and P. Kim, Phys. Rev. Lett. **98**, 206805 (2007).
9. C. Jeong, P. Nair, M. Khan, M. Lundstrom, and M.A. Alam, Nano Lett. **11**, 5020 (2011).
10. K. Wakabayashi, M. Fujita, H. Ajiki, and M. Sigrist, Phys. Rev. B **59**, 8271 (1999).
11. J. Cai, P. Ruffieux, R. Jaafar, M. Bieri, T. Braun, S. Blankenburg, M. Muoth, A.P. Seitsonen, M. Saleh, X. Feng, K. Muellen, and R. Fasel, Nature **466**, 470 (2010).
12. R.M. Balabai and N.V. Grishchenko, Fotoelektronika **8**, 25 (1998).
13. R.M. Balabai, *First-Principles Computational Methods in Solid State Physics: The Quantum-Mechanical Molecular Dynamics* (Vydavnychyi Dim, Kryvyi Rih, 2009) (in Ukrainian).
14. D.W. Boukhvalov and M.I. Katsnelson, J. Phys. Condens. Matter **21**, 344205 (2009).
15. V. Litovchenko, Ukr. Fiz. Zh. **42**, 228 (1997).
16. V.G. Litovchenko, M.V. Strikha, and N.I. Klyui, Ukr. Fiz. Zh. **56**, 178 (2011).
17. R.M. Balabai and D.V. Ryabchikov, Sensor. Elektron. Mikrosyst. Tekhnol. **2**, N 8, 13 (2011).
18. M.M. Brzhezinskaya, A.S. Vinogradov, A.V. Krestinin, A.P. Kharitonov *et al.*, Fiz. Tverd. Tela **52**, 819 (2010).

Р.М. Балабай

ЕЛЕКТРОННІ ВЛАСТИВОСТІ ФУНКЦІОНАЛІЗОВАНИХ ГРАФЕНОВИХ НАНОСТРІЧОК

Р е з ю м е

Методами функціонала електронної густини та псевдопотенціалу із перших принципів отримані розподіли густини валентних електронів та електронні енергетичні спектри для графенових наностічок, декорованих воднем, фтором або киснем. Продемонстровано відкриття забороненої зони для графенових наностічок шириною в 9,23 Å із зигзагоподібним краєм, за її відсутності у необмеженій графеновій площині. Заборонена зона зі збільшенням ширини графенових наностічок зменшується. Для графенових наностічок, декорованих по краях воднем, заборонена зона зникає. Продемонстровано, що взаємодія атомів водню з атомами вуглецю площини графенових наностічок, що координовані відповідно до sp^2-гібридизації, приводить до локальних змін гібридизації до типу sp^3.